Numerical studies of the dynamics of multiphoton processes with arbitrary field polarization: Methodological considerations

Etienne Huens and Bernard Piraux
Institut de Physique, Université Catholique de Louvain, 2, Chemin du Cyclotron, B1348 Louvain-La-Neuve, Belgium

Alejandro Bugacov
Physics Department, University of Southern California, Los Angeles, California 90089-0484

Mariusz Gajda
Polish Academy of Sciences, Institute of Physics and College of Science, Aleja Lotników 32/46, 02 668 Warsaw, Poland
(Received 30 May 1996)

We describe an approach of spectral type for numerically integrating the time-dependent Schrödinger equation associated to the interaction of a one active electron atom with an electromagnetic pulsed field whose polarization may be arbitrary. The wave function is represented on a Coulomb-Sturmian basis. The time propagation method is based on a parallel-iterated Runge-Kutta method of predictor-corrector type. This method is in fact fully implicit and of very high order, ensuring a high stability of the time propagation. Moreover, it has the following advantages: it provides a scheme for an adaptive time step and it is particularly well suited to parallel computing. We discuss the performance of the present approach and compare it to already existing ones. In the case of linearly polarized fields, most of our results are in good agreement with those obtained with other approaches. In the case of circularly polarized fields, we compare our results with those obtained by, so far, the only existing method which is based on the single state Floquet approximation. Finally, and for the sake of illustration, we treat the case of the interaction of atomic hydrogen with a strong pulsed electromagnetic field whose polarization depends on time. [S1050-2947(97)02902-8]

PACS number(s): 32.80.Rm, 42.65.Ky

I. INTRODUCTION

The role of numerical simulations is now becoming increasingly important in the study of the dynamics of a broad spectrum of complex physical processes [1]. Multiphoton processes resulting from the interaction of an atom with a pulsed electromagnetic field are typical examples [2]. Indeed, given the short time scales over which these phenomena can now be observed, it is expected that tremendous insight may be gained by following their entire time evolution. Furthermore, simulations based on the direct numerical integration of the Schrödinger equation turned out to be extremely useful in predicting new effects such as, for instance, the adiabatic stabilization of a one-electron system in a strong pulsed high frequency laser field [3].

Considerable efforts have been put into the development of numerical methods to solve the time-dependent Schrödinger equation associated to the interaction of a one- and even two-electron system with a strong pulsed electromagnetic field. Although it is undeniable that some of these methods are extremely efficient, it is clear, however, that the amount of computational effort imposes serious limitations to their domain of applicability even in the case of a one-electron system. The interaction of a one-electron system with a circularly or elliptically polarized pulsed field is only one among various examples. The purpose of the present contribution is twofold. First, we show that many of the problems related to stability, time step control, and hence accuracy and speed of the time propagation procedure used in many of the already existing methods may be solved by introducing a recent advanced algorithm [4]. We then study for the sake of illustration the ionization of atomic hydrogen by a strong ultrashort electromagnetic pulse whose polarization depends on time. Besides this example, it is worth mentioning that the present approach has been successfully applied to the study of the interaction of a Rydberg atom with both a linearly polarized half-cycle pulse [5] and a circularly polarized microwave pulse [6].

There are basically two types of methods to solve numerically the time-dependent Schrödinger equation: grid [7] and spectral methods [8]. Schematically, grid methods consist in time propagating the total wave function defined in terms of its finite difference representation on a spatial grid. Usually, the time propagation is carried out by means of a second order implicit scheme which allows the time propagator to be expressed in terms of tridiagonal matrices [9]. In that case, the calculations are greatly simplified and the computational effort is linear in the total number of grid points (given in the case of a linear polarized field by the product of the number of angular momentum values and the number of radial grid points). The final state distribution for the electron both within the bound state manifold and in the continuum is easily obtained from the knowledge of the wave function at the end of the interaction with the pulse. This type of method revealed itself very efficient and provided many results [10] [concerning the ionization yield, the electron above-threshold ionization (ATI) spectra, the harmonics spectra, etc.] in the case of the interaction of a linearly polarized field with a one-electron system initially in its ground state or a low excited state. According to the previous discussion, it is clear, however, that if the initial state is a high lying state or if the field is circularly or elliptically polarized, the size of

the grid as well as the number of grid points is expected to increase dramatically, making the problem very difficult.

Spectral type methods consist in expanding the total wave function in a basis of functions which, usually, are L^2-*integrable* for the radial coordinates and spherical harmonics for the angular coordinates. The total wave function is then propagated in time by means of either an explicit or implicit scheme [11]. Here, we stress that by contrast to what is usually written in the literature, the computational effort is not necessarily proportional to the third power of the number of basis functions which if it turned out to be the case, would lead to unmanageably large calculations. In fact, we show in this contribution that with a proper choice of the basis of L^2-*integrable* functions and of the time integration scheme, the computational effort is drastically reduced and scales as the first power of the total number of basis functions which, in the same time, can be significantly decreased when complex scaling methods are used.

The paper is organized as follows: we first start by formulating the problem with some emphasis on the basis used to expand the full wave function of the system. Then, we discuss and show how to optimize the choice of a particular Sturmian basis. The fourth section is devoted to the time propagation method. In particular, we show why this method is appropriate for parallel computing and why it provides a very good scheme for an adaptative time step. The calculation of various observables is described in the next section. We then compare some of our results with those obtained by other existing methods for both linearly and circularly polarized fields. Finally, for the sake of illustration, we treat briefly the problem of the interaction of atomic hydrogen with a strong pulsed electromagnetic field whose polarization depends on time.

II. FORMULATION AND PRELIMINARY REMARKS

The time evolution of the wave function $\Psi(\vec{r},t)$ describing a hydrogenic system interacting with a pulsed electromagnetic field is given by the Schrödinger equation which reads (unless stated, we use atomic units and the Gaussian system for the fields)

$$i\frac{\partial}{\partial t}\Psi(\vec{r},t)=H(\vec{r},t)\Psi(\vec{r},t), \tag{1}$$

where H is the total Hamiltonian defined as the sum of $H_{\rm at}$ and $H_{\rm int}$, the atomic and interaction Hamiltonian, respectively. Within the dipole approximation (and provided that no further approximation is made), the interaction Hamiltonian $H_{\rm int}(\vec{r},t)$ may be written in two equivalent forms: either in its *velocity* form denoted by $H^V_{\rm int}(\vec{r},t)$ or in its *length* form denoted by $H^L_{\rm int}(\vec{r},t)$:

$$H^V_{\rm int}(\vec{r},t)=\frac{1}{c}\vec{A}(t)\cdot\vec{p}, \tag{2}$$

$$H^L_{\rm int}(\vec{r},t)=\vec{E}(t)\cdot\vec{r}, \tag{3}$$

c is the speed of light. The electric field $\vec{E}(t)$ is related to the vector potential $\vec{A}(t)$ by the usual relation $\vec{E}(t)=-(1/c)(d/dt)\vec{A}(t)$. Note that since $\vec{A}(t)$ does not depend on $\vec{r}$, we do not take into account in Eq. (2) the term proportional to A^2 which can be eliminated from the total Hamiltonian by a phase transformation of the wave function $\Psi(\vec{r},t)$. Here, we assume that the electric field lies in the x-y plane. The corresponding vector potential is defined as

$$\vec{A}(t)=A_1 f_1(t)\cos(\omega_1 t+\phi_1)\vec{\epsilon}_x+A_2 f_2(t)\sin(\omega_2 t+\phi_2)\vec{\epsilon}_y, \tag{4}$$

where A_1, f_1, ω_1, and ϕ_1 are, respectively, the amplitude, the pulse envelope, the frequency, and the initial phase of the x component of the vector potential; the same quantities with index 2 correspond to the y component. When $\omega_1=\omega_2$, the polarization of the field may be linear, circular, or elliptical depending on the value of A_1, A_2, ϕ_1, and ϕ_2. Time-dependent polarization may be obtained for instance, when ω_1 is close but different from ω_2.

In order to solve Eq. (1), we now expand the total wave function on a discrete set of L^2-*integrable* functions $F_{n,l}(r)$ for the radial coordinate r and spherical harmonics $Y_{l,m}(\hat{r})$ for the angular coordinate $\hat{\vec{r}}$:

$$\Psi(\vec{r},t)=\sum_{n,l,m} a_{n,l,m}(t)F_{n,l}(r)Y_{l,m}(\hat{\vec{r}}). \tag{5}$$

This transforms Eq. (1) into a set of coupled ordinary differential equations for the coefficients $a_{n,l,m}(t)$. The choice of the basis of L^2-*integrable* functions $F_{n,l}(r)$ is crucial in order to keep the computational effort within reasonable limits. The system of equations should be sparse and banded, with the smallest possible bandwidth. Various types of L^2-*integrable* functions have been used so far: essentially spline [12], and Sturmian functions [13]. In the case of atomic hydrogen, the Sturmian functions are the most appropriate ones to meet the above requirement since the matrix associated to the atomic Hamiltonian is tridiagonal [14] while each block of the block matrix associated to the interaction Hamiltonian is either bidiagonal for $H^V_{\rm int}$ or pentadiagonal for $H^L_{\rm int}$. Furthermore, all matrix elements may be written in a very simple compact analytical form (see the Appendix). The reason for these properties of the Sturmian functions comes essentially from the fact that these functions denoted by $S^\kappa_{n,l}(r)$ are actually eigenfunctions of the radial *hydrogenic* Sturm-Liouville eigenvalue problem [15]:

$$\left(-\frac{1}{2}\frac{d^2}{dr^2}+\frac{l(l+1)}{2r^2}-\frac{\alpha}{r}+\frac{\kappa^2}{2}\right)S^\kappa_{n,l}(r)=0, \tag{6}$$

with the boundary conditions $S^\kappa_{n,l}(0)=S^\kappa_{n,l}(\infty)=0$. In the above equation, the *coupling constant* α is the eigenvalue equal to κn and the energy $(-\kappa^2/2)$ is fixed and negative ensuring the discreteness of the eigenvalue spectrum. n is a positive integer always larger than l (the angular momentum quantum number) and related to the number of nodes of $S^\kappa_{n,l}(r)$. As for hydrogenic wave functions, the Sturmian functions may be expressed in terms of confluent hypergeometric functions as follows:

$$S^\kappa_{n,l}(r)=N^\kappa_{n,l}r^{(l+1)}e^{-\kappa r}{}_1F_1(-n+l+1;2l+1;2\kappa r), \tag{7}$$

where $N_{n,l}^{\kappa}$ is a normalization factor. Note that in order to ensure the right behavior of $\Psi(\vec{r},t)$ at the origin, we must write $F_{n,l}(r)=S_{n,l}^{\kappa}(r)/r$ in Eq. (5). Before discussing the Sturmian functions any further, it is worth mentioning that banded matrices are also obtained with spline functions, the number of bands depending on the degree of the spline function. In general, one has to use rather high order spline functions to obtain a reasonable accuracy so that the matrices associated to the full Hamiltonian operator are less sparse than in the case of Sturmian functions. However, the spline functions offer the advantage of leading to sparse matrices for any type of potential (not necessarily Coulombic as in the case of Sturmian functions). Moreover, by contrast to the Sturmian functions, the spline functions are not necessarily ''localized'' around the origin [16]; this may be of interest in calculating electron energy spectra [17].

If the Sturmian basis were infinite, the choice of the wave number κ would be irrelevant. In practice, the size of the basis is finite and it is therefore important to choose the value of κ in order to make the basis the most adapted one to the physical situation in hand. For instance, we see from Eq. (6) that in the case where high excited states play an important role in the physical process, the value of κ should be rather small since solutions of Eq. (6) for small κ and hence small energies represent states which have the same behavior as Rydberg hydrogenic states. We discuss in detail how to optimize both κ and the size of the basis in the next section.

Although κ has been assumed real so far, nothing prevents us from making κ complex in Eq. (7). This has in fact important consequences [18]. It allows the basis function to have an asymptotic behavior which is suited to the physical boundary conditions of the problem [19]. Indeed, by choosing the wave number κ in the lower right quadrant of the complex plane, the factor $e^{-\kappa r}$ has the character of both closed channel and outgoing wave open channel function. If κ were chosen real, the basis would have only the character of closed channels. As a result, the norm of the total wave function would be conserved in time. In other words, because of the L^2 *integrability* of the basis functions, such a basis would describe the system over a restricted region of space, say, a sphere of some characteristic radius [20]. Hence any probability density flux reaching the surface of the sphere over the time interval of interest would reflect from the surface and return to the interior of the sphere. Such a spurious reflection, which is a common problem for all spectral methods (as well as grid methods), can of course be avoided by enlarging the basis (or the grid size). However, we can instead use complex basis functions which effectively make the surface of the sphere an absorbing wall. Indeed, on a complex basis, the norm of the wave function is not conserved but instead represents at long asymptotic times the probability for the system to stay bound [21]. In practice, this means that the size of the Sturmian basis does not need to be excessively large since it is supposed to describe properly the system inside the sphere only. Typical values of N_s, the number of basis functions needed per angular momentum, are given in Sec. VII where we discuss an example.

A serious numerical problem common to all spectral methods is the so-called *stiffness* of the system of equations satisfied by the coefficient $a_{n,l,m}$. In practice, it means that if we use a standard explicit method to time propagate the solution, one has to decrease the time step if the number of equations (in other words, the number of basis functions) is increased. This of course represents a severe limitation of the explicit time propagation methods. Physically, the origin of the stiff character of the system of equations satisfied by the coefficients $a_{n,l,m}$ may be explained as follows: let us suppose that having expanded the total wave function $\Psi(\vec{r},t)$ in the Sturmian basis we switch to the atomic basis in which the matrix associated to the atomic Hamiltonian $H_{\rm at}$ is diagonal. Since the size of the discrete basis is finite, the spectrum of this matrix contains a finite number of negative energy eigenvalues and a finite number of positive ones which may be very high. The value of the highest ones increases when both κ and N_s, the number of Sturmian functions per angular momentum l, increase. Now, in the atomic basis, the total wave function $\Psi(\vec{r},t)$ is written as follows:

$$\Psi(\vec{r},t)=\sum_{l,m}\left\{\sum_{n} b_{n,l,m}(t)R_{n,l}(r) + \sum_{i} b_{E_i l,m}(t)R_{E_i l}\right\}Y_{l,m}(\hat{\vec{r}}), \tag{8}$$

where $R_{n,l}$ and $R_{E_i,l}$ are the radial bound and continuum hydrogenic eigenstate wave functions taken into account. The amplitudes $b_{E_i,l,m}(t)$ may be written as $b_{E_i,l,m}(t)=\tilde{b}_{E_i,l,m}(t)e^{-iE_i t}$ and similarly for the bound state amplitudes $b_{n,l,m}(t)$. Note that unless the coupling with the external field is very strong, $\tilde{b}_{E_i,l,m}$ varies smoothly with time. Therefore we expect that the time step should be at least smaller than $1/E_{\rm max}$ where $E_{\rm max}$ is the highest energy eigenvalue. On the other hand, in most of the physical situations, the very high energy eigenvalues do not play any role and it is perfectly safe to drop the corresponding amplitudes from expansion (8). One has, however, to stress that if one works in the atomic basis, the matrix associated to the interaction Hamiltonian is full, causing storage problems and increasing significantly the computational effort. Since a given Sturmian function may be expressed as a linear superposition of atomic wave functions, it is clear that each of the expansion coefficients $a_{n,l,m}(t)$ will contain many rapidly oscillating components which by contrast to the atomic basis cannot be eliminated. The only way to solve this problem is to use an implicit time propagation scheme. This problem is treated in detail in Sec. IV. Meanwhile, let us examine in the next section some properties of the Sturmian basis and how it is possible to choose κ and N_s to make the basis the most adapted one to the physical situation in hand.

III. OPTIMAL CHOICE OF A STURMIAN BASIS

As we saw before, the expansion (5) leads to a discretized spectrum of the atomic Hamiltonian. For each angular momentum l, this spectrum contains N_s^b negative eigenenergies and N_s^c positive ones. To each of these eigenenergies corresponds an eigenstate wave function which may be written as a linear superposition of a finite number of Sturmian functions. Among the N_s^b bound eigenstate wave functions, $\tilde{N}_s^b$

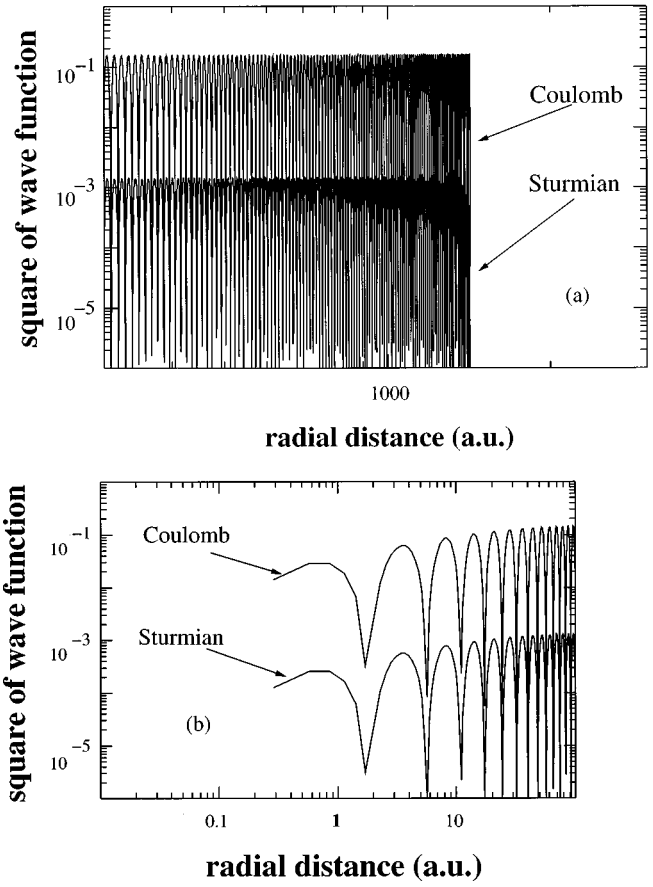

FIG. 1. Square of the radial Coulomb wave function of angular quantum number $l=0$, for an energy of 0.0497 a.u. as a function of the radial distance in a.u. This function is compared to the corresponding superposition of Sturmian functions of κ parameter equal to 0.5 a.u., the number of Sturmian functions N_s being equal to 500; (a) large scale behavior, and (b) behavior around the origin. Note that in (a), the curve associated to the radial Coulomb function is truncated where the corresponding superposition of Sturmian functions vanishes.

coincide within the accuracy of the computer, with the exact hydrogenic eigenstate wave functions. Similarly, for each positive eigenenergy, the associated eigenstate wave function reproduces, within a normalization constant, the corresponding radial Coulomb function. In Fig. 1 we compare the radial Coulomb function for an energy $E=0.0497$ a.u. with the corresponding superposition of Sturmian functions; in this case, the angular momentum quantum number $l=0$, the κ parameter is equal to 0.5 a.u., and $N_s=500$. We clearly see that up to a radial distance of about 1000 a.u., both the Coulomb function and its corresponding superposition of Sturmian functions differ only by a normalization factor. Beyond this radial distance of 1000 a.u., the superposition of Sturmian functions goes to zero rapidly due to their L^2-*integrable* character while the Coulomb function extends to the infinity. The question we address in this section is the following: what are, for a given physical situation, the values of κ and N_s leading to an appropriate distribution of the positive eigenvalues required for the calculation of the electron energy spectrum while keeping $\tilde{N}_s^b$ sufficiently large.

Before examining this question in detail, let us recall some of the basic properties of the Sturmian functions [22]. The Sturmian functions which are solution of the eigenvalue problem (6) satisfy the orthogonality relation:

$$\langle S_{n,l}^{\kappa}|S_{n',l}^{\kappa}\rangle \equiv \int_0^{\infty} S_{n,l}^{\kappa}(r)\frac{1}{r}S_{n',l}^{\kappa}(r)dr=0, \quad n\neq n'. \tag{9}$$

In the following, we assume that these functions are normalized in such a way that the diagonal elements of the overlap matrix **S** are equal to unity. This matrix is in fact symmetric and positive definite. In the Sturmian basis, and with the above convention, the matrix $\mathbf{H}_{\rm at}$ associated to the atomic Hamiltonian $H_{\rm at}$ may be expressed in terms of the overlap matrix **S** as follows:

$$\mathbf{H}_{\rm at}=\kappa^2\mathbf{I}-\kappa\mathbf{N}-\frac{\kappa^2}{2}\mathbf{S}, \tag{10}$$

where **N** is a diagonal matrix whose elements are $1/n$ and **I** the unit matrix.

In the Sturmian basis, the eigenvalues of the atomic Hamiltonian are obtained by solving the following generalized eigenvalue problem:

$$(\mathbf{H}_{\rm at}-E\mathbf{S})\mathbf{\Phi}=\mathbf{0}, \tag{11}$$

where E is the eigenvalue and $\mathbf{\Phi}$ the eigenvector. This problem may be easily solved by using Eq. (10). Let us mention, however, that if we are only interested in the distribution of the eigenvalues, i.e., in the number of eigenvalues whose value belongs to a given interval, there is no need to solve the above system. Instead, we can use Dean's algorithm which provides the number of eigenvalues less than a given number in the case of a symmetric matrix [23]. Let us now examine how the number of negative eigenvalues varies with κ and N_s. The results are presented for $l=0$ in Fig. 2 where we give the number of negative eigenvalues as a function of κ for various N_s. As we see, there are striking regularities that we can exploit to extract an empirical formula. We find that the number of negative eigenvalues is given by

$$N_s^b=\max\left(N_s;1.22\sqrt{\frac{N_s}{\kappa}}\right). \tag{12}$$

Note that if κ is complex, it should be replaced by its real part in the above formula. This formula has been checked for a wide range of values of κ (from 0.01 to 1 in a.u.) and N_s (from 50 to 500). In all cases, the error between the exact number of negative eigenvalues and the estimated result given by Eq. (12) is extremely small. One might wonder whether or not this result could be derived analytically. In fact one knows that there is a relation between the position of the eigenvalues E and the location of the zeros of Pollaczek's polynomials [14]. However, as far as we know, the existence of an analytical expression for the calculation of the zeros of Pollaczek' polynomials is still an open question [24]. On the other hand, it turns out that in all cases, 75% of the negative eigenvalues coincide with the exact hydrogenic eigenvalues within less than 1%. Finally, let us mention that, although not reproduced here, a similar study may be carried out for $l\neq 0$.

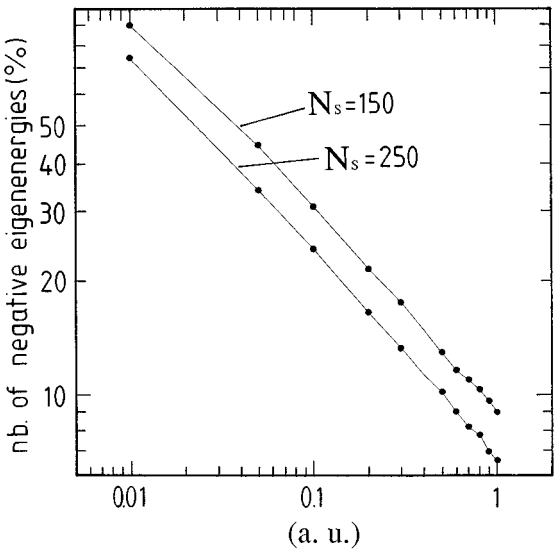

FIG. 2. Percentage of negative eigenenergies of atomic hydrogen resulting from the diagonalization of the corresponding Hamiltonian matrix calculated in a basis of Sturmian functions. This percentage is plotted as a function of the Sturmian κ parameter for two different values of N_s, the number of Sturmian functions used in the basis. We assume that the angular quantum number l is equal to 0; similar results are obtained for different values of l.

Let us now examine the distribution of the positive eigenvalues. In Fig. 3 we show the position of the positive eigenvalues for various κ parameters; the angular quantum number $l=0$ and $N_s=250$. First, we see that the number of eigenenergies increases with κ and secondly, it is clear that the distribution shifts towards higher energies when κ increases. It is convenient to introduce the following quantity

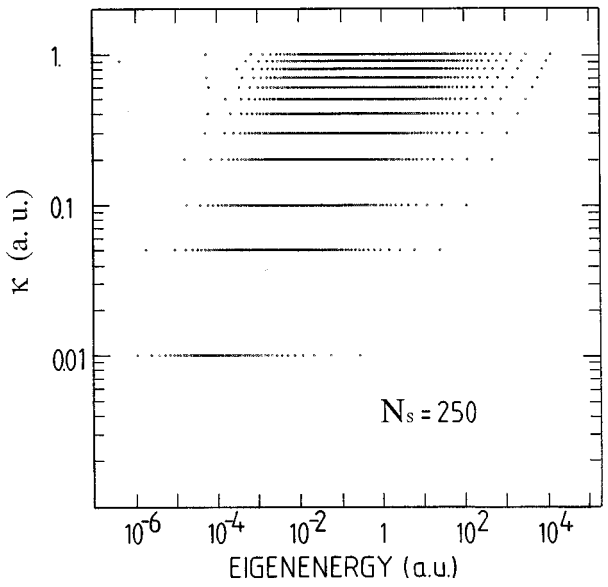

FIG. 3. Positive eigenenergies in a.u. of atomic hydrogen resulting from the diagonalization of the corresponding Hamiltonian matrix calculated in a basis of Sturmian functions. These eigenenergies are plotted for various values of the Sturmian κ parameter. As in the previous figure, the angular quantum number l is assumed to be 0. N_s, the total number of Sturmian functions, is equal to 250.

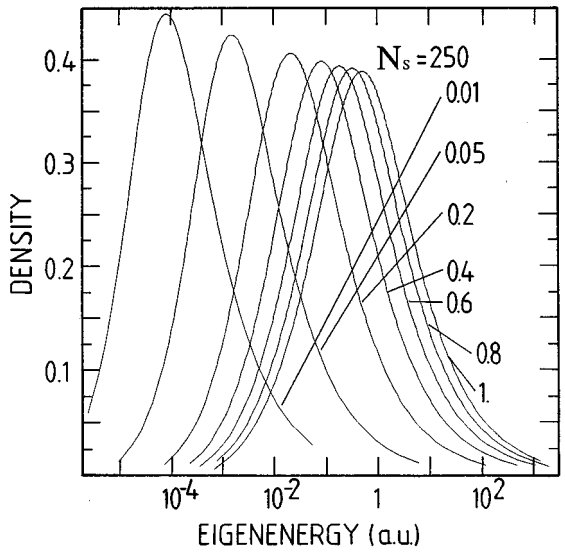

FIG. 4. Density of positive eigenenergies for various values of the Sturmian κ parameter for the same case as in Fig. 3.

denoted by D which may be interpreted as a measure of the density of positive eigenenergies:

$$D=\frac{1}{\ln(E_{i+1}/E_i)}. \tag{13}$$

This quantity D as a function of the eigenenergies E_i is plotted in Fig. 4 for various values of κ and for $N_s=250$. As in Fig. 3, we clearly see that the maximum of this density shifts towards larger energies as κ increases. Moreover, Fig. 5 indicates that the energy corresponding to the maximum of this density is a linear function of κ in a log-log plot. The reason for this striking behavior is still an open question.

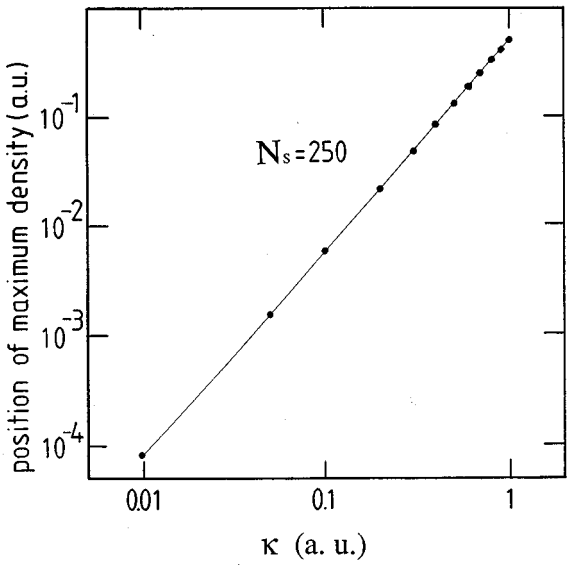

FIG. 5. Position of the maximum density in a.u. of positive eigenenergies as a function of the Sturmian κ parameter for the same case as in Figs. 3 and 4.

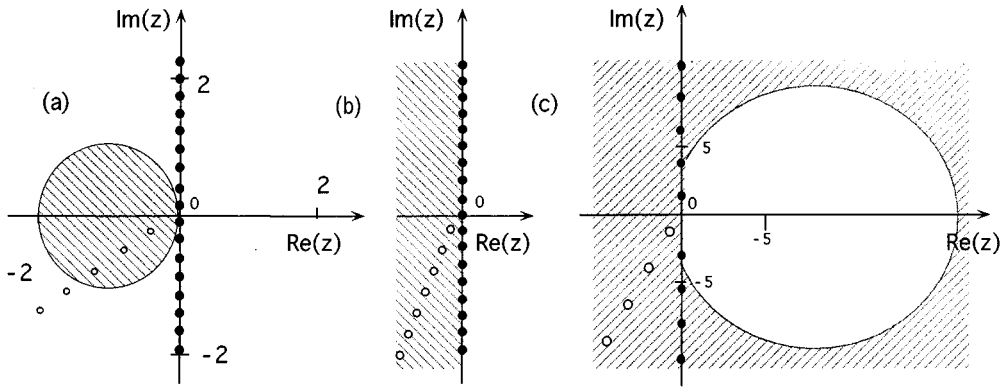

FIG. 6. Typical behavior of the stability function $R(Z)$ in the Z-complex plane. The hatched zones correspond to $|R(Z)|<1$. Outside these zones, $|R(Z)|>1$ and at the border, $|R(Z)|=0$. This stability function is associated to a given Runge-Kutta method. Three cases are considered: (a) an explicit method, (b) an implicit method of Gauss type, and (c) an implicit method of non-Gauss type.

IV. TIME PROPAGATION METHOD

In the Sturmian basis, the Schrödinger equation we have to solve may be written as follows:

$$i\frac{d}{dt}\mathbf{S}\Psi(t)=\mathbf{H}(t)\Psi(t), \tag{14}$$

where Ψ is a vector which contains the coefficients $a_{n,l,m}$; $\mathbf{H}$ is a block tridiagonal matrix associated to the total Hamiltonian. The diagonal blocks are tridiagonal and correspond to the atomic Hamiltonian. The off-diagonal blocks correspond to the interaction Hamiltonian: they are either bidiagonal in the case of $H^V_{\rm int}(\vec{r},t)$ or pentadiagonal in the case of $H^L_{\rm int}(\vec{r},t)$. Details about the expression of the corresponding matrix elements may be found in the Appendix. As we mentioned in Sec. II, the above system is *stiff*, requiring an implicit scheme to time propagate the solution. The procedure which is briefly described here has been developed by van der Houwen and Sommeijer [25]; it is of *predictor-corrector* type and is based on implicit Runge-Kutta methods.

The general Runge-Kutta method to propagate the solution of Eq. (1) over a time step h from, say, t_n until t_{n+1} is given by

$$\Psi(t_{n+1})=\Psi(t_n)-ih\sum_{i=1}^{s} b_i\mathbf{S}^{-1}\mathbf{H}(t_i)\Psi(t_i), \tag{15}$$

$$\Psi(t_i)=\Psi(t_n)-ih\sum_{j=1}^{s} a_{ij}\mathbf{S}^{-1}\mathbf{H}(t_j)\Psi(t_j), \quad i=1,\ldots,s. \tag{16}$$

b_i and a_{ij} are the coefficients defining the Runge-Kutta method; s, the number of mesh points t_i, is called the number of stages. $\Psi(t_i)$ is the state vector at time t_i. A Runge-Kutta method is said to be explicit if $a_{ij}=0$ for $j\geqslant i$. It is said to be diagonally implicit if $a_{ij}=0$ for $j>i$ and fully implicit in all other cases. If the method is explicit, the $\Psi(t_i)$ are not coupled in Eq. (16) and can be obtained by simple matrix vector multiplications. In the case of implicit methods, on the other hand, the vector Ψ at time t_i is obtained by solving large systems of linear equations. For diagonally implicit methods, one has to solve s systems of dimension N where N is the total number of Sturmian functions, while for a fully implicit method only one system has to be solved, but of dimension sN.

Before discussing our specific choice of the Runge-Kutta methods for the predictor and the corrector, it is interesting to briefly analyze the behavior of the so-called stability function associated to a given Runge-Kutta method. For the sake of illustration, we consider the following standard test problem:

$$\frac{d\mathbf{Y}}{dt}=\lambda y, \quad \mathrm{Re}(\lambda)\leqslant 0. \tag{17}$$

Equation (14) reduces to the above equation if we assume the vector potential $\vec{A}(t)$ constant and if the total Hamiltonian is diagonal. Under these conditions, one can show that [26]

$$\mathbf{Y}(t_{n+1})=R(Z)\mathbf{Y}(t_n), \tag{18}$$

where Z is defined as the product of λ and the time step $h=t_{n+1}-t_n$. $R(Z)$, called the stability function, is defined as follows:

$$R(Z)=\frac{\det[\mathbf{1}-Z\mathbf{A}+Z\mathbf{e}\mathbf{b}^T]}{\det[\mathbf{1}-Z\mathbf{A}]}. \tag{19}$$

$\mathbf{A}$ is a matrix whose elements are the $a_{i,j}$ and $\mathbf{b}$ a vector whose components are the b_i coefficients [see Eqs. (15) and (16)], $\mathbf{1}$ is the unit matrix, and $\mathbf{e}=(1,1,1,\ldots,1)^T$. As a result, we see that the norm of vector $\mathbf{Y}$ is conserved when $|R(Z)|=1$ (in this case, we assume that the basis functions are real). Furthermore,

$$|R(Z)|>1 \rightarrow \lim_{n\rightarrow\infty}\mathbf{Y}(t_n)=\infty, \tag{20}$$

$$|R(Z)|<1 \rightarrow \lim_{n\rightarrow\infty}\mathbf{Y}(t_n)=0. \tag{21}$$

Figure 6 shows the typical behavior of $R(Z)$ in the Z-complex plane for three cases: (a) an explicit method and (b), (c), two implicit methods. The hatched zones are characterized by $|R(Z)|<1$, outside the this zone, $|R(Z)|>1$ and

at the border, $|R(Z)|=1$. The full dots give the position of $h\lambda$ when the basis is real. Note that because of factor i in Eq. (14), λ is purely imaginary. The empty dots give the position of $h\lambda$ when the basis is complex. In Fig. 6(a), we examine the case of an explicit scheme; according to the previous discussion and given the position of $h\lambda$, it is clear that the only way to conserve the norm when the basis is real is to impose a time step h going to zero. In practice, the time step is finite. Therefore, since there are always values of $h\lambda$ on the positive imaginary axis, the solution will diverge after a while. In Fig. 6(b), we consider the case of an implicit Runge-Kutta method of Gauss type (characterized by the fact that the order of the method is twice the number of mesh points). A typical example is the widely used Cranck-Nicholson algorithm [27]. If the basis is real, we see that the norm of vector $\mathbf{Y}$ is always conserved. If the basis is complex, the norm decreases as expected. However, one has to be very careful because, as we experienced, the time step h has to be very small to ensure a reasonable accuracy if the order of the method is low as for the Cranck-Nicholson method. Finally, in Fig. 6(c), we analyze the case of a high order implicit Runge-Kutta method (of non-Gauss type). We see that the norm is not necessarily conserved if the basis is real, but on the other hand, it is clear that the time step does not need to be so small to ensure a reasonable accuracy.

In the present case, it is sufficient to use a two-point diagonally implicit method for the predictor [28]. For the corrector, we use a four-point fully implicit method of Runge-Kutta type which is of order 7. In order to avoid the high cost of solving a large system of dimension $4N$, we used a method developed by van der Houwen and Sommeijer and which exploits parallelism across the method [25]. It consists in solving the large system of algebraic equations iteratively; at each iteration, one has to solve four systems of dimension N which, being independent, may be solved in parallel. Note that this procedure does not work when the Runge-Kutta method is of Gauss type. The systems are solved by means of the biconjugate gradient algorithm [29]. In the present case, this algorithm, which is iterative, converges quickly after fewer than ten iterations regardless of the size of the basis. This, with the fact that the matrix associated to the full Hamiltonian is sparse, explains why the number of operations grows only linearly with the size of the basis.

Besides the parallelism across the method, this time propagation algorithm provides a scheme for a step size control based on the speed of convergence v_c of the iterative procedure: after having propagated with a given time step from say t_i to t_{i+1}, we calculate the next step size by multiplying the previous one by an appropriate factor which depends on v_c. This procedure has been tested in many different physical situations, and turned out to be crucial in order to optimize the execution time, while keeping the accuracy at a reasonable level. It has to be stressed that the problem of the choice of the time step is difficult; indeed, in many cases, it is impossible to define its magnitude *a priori*. If the system, for instance, emits high harmonics of the driving field at the beginning of the interaction, then the step size has to be at least smaller than the period of the highest order harmonic though the field intensity is not necessarily very high [30].

V. OBSERVABLES

After the time propagation, the solution $\Psi(\vec{r},t)$ of Eq. (1) has to be projected on the atomic basis. We proceed as follows: since $\mathbf{S}$, the overlap matrix, is symmetric and positive definite, we can perform a Choleski decomposition of $\mathbf{S}$:

$$\mathbf{S}=\mathbf{L}\mathbf{L}^T, \tag{22}$$

where $\mathbf{L}$ is a lower triangular matrix with only two nonzero bands, the diagonal and the first subdiagonal. In these conditions the generalized eigenvalue problem (11) may be rewritten in the following way:

$$\left[\mathbf{L}^T\left(1-\frac{1}{\kappa N_s}\right)^{-1}\mathbf{L}\right](\mathbf{L}^T\boldsymbol{\xi})=\lambda(\mathbf{L}^T\boldsymbol{\xi}). \tag{23}$$

The matrix between large parentheses on the left hand side of the equation is tridiagonal and symmetric. λ, the eigenvalue, is related to the atomic eigenenergy E by

$$\lambda=\frac{1}{E/\kappa^2+\frac{1}{2}}. \tag{24}$$

Having found the eigenvectors $\mathbf{L}^T\xi$ of Eq. (23), it is easy to show that $\mathbf{\Psi}_{\rm at}$, the state vector in the atomic basis, may be obtained from $\mathbf{\Psi}_{\rm st}$, the state vector in the Sturmian basis, by using the following relation:

$$\mathbf{\Psi}_{\rm at}=\mathbf{Y}^T\mathbf{L}^T\mathbf{\Psi}_{\rm st}, \tag{25}$$

where $\mathbf{Y}$ is the matrix whose columns are the eigenvectors $\mathbf{L}^T\xi$. This simple procedure is valid whether or not the basis is real or complex. The coefficients of the state vector $\mathbf{\Psi}_{\rm at}$ are the amplitudes $b_{n,l,m}$ for the bound states and $b_{E_i,l,m}$ for continuum states as defined in Eq. (8). $|b_{n,l,m}|^2$ represents the probability for the system to be in the n,l,m state. If the basis is complex, this result is still valid and one minus the sum of all these probabilities is of course the ionization yield. If the basis is real, $|b_{E_i,l,m}|^2$ represents the probability for the system to be in a continuum state of angular momentum l, azimuthal quantum number m, and energy E between E_i and E_{i+1}. As a result, the electron energy spectrum $P(E)$ which represents a probability density may be calculated as follows:

$$P(E)=\frac{|b_{i+1,l,m}|^2}{E_{i+1}-E_i}, \quad E_i<E\leqslant E_{i+1}. \tag{26}$$

It is important to note that knowing the state vector $\mathbf{\Psi}(t)$ in any basis (Sturmian or atomic), we are able to compute the expection value of any physical observable. This is true whether or not the basis is real. However, if it is complex, one has to use analytical continuation techniques like the Padé approximants to get convergence when the contributions of all components of $\mathbf{\Psi}(t)$ and especially the continuum ones, are summed up. This remark is of course crucial for the calculation of electron energy spectra with a complex basis [21]. By contrast, the use of a complex basis to calculate the acceleration of the dipole does not lead to particular problems since in this case the dominant contribution comes in general from lower lying bound states.

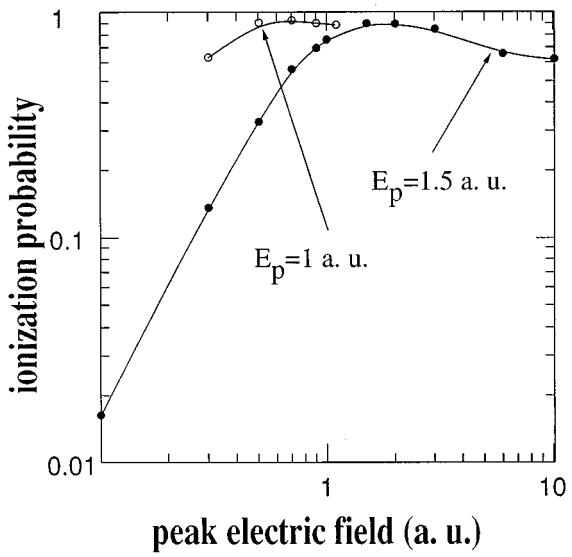

FIG. 7. Ionization probability as a function of the peak electric field in a.u. resulting from the interaction of atomic hydrogen with a sharply turned on and off (step function) linearly polarized electromagnetic pulse of duration equal to ten optical cycles. Atomic hydrogen is assumed initially in its ground state and we consider two photon energies E_p: 1 a.u. and 1.5 a.u.

VI. COMPARISON WITH OTHER CALCULATIONS

In the case of linear polarization, where comparison is possible, our results agree with those obtained by means of grid methods as developed by Kulander [31]. In a recent paper about adiabatic stabilization of atomic hydrogen exposed to a strong field, Kulander *et al.* [3] mentioned that stabilization cannot be achieved when the electric field is sharply turned on (turn-on time less than five optical periods). This seems, however, to disagree with our results shown in Fig. 7 where the ionization yield is shown as a function of the peak electric field for two different photon energies (1 a.u. and 1.5 a.u.), the time profile of the electric field being a step function. Since the amount of population trapped in excited states is rather significant as expected (about 22% of the total population in the case where $\omega=1$ a.u.), we expect that, in the presence of a strong high frequency electric field, those excited states should easily stabilize.

In the case of circular polarization, no other time-dependent calculations exist as far as we know. However, it is interesting to compare our results with independent Floquet type calculations performed by Zakrzewski and Delande [32]. These results are presented in Fig. 8 where ionization yields are shown as a function of the peak electric field in atomic units for the following case: atomic hydrogen is initially in the $n=2$, $l=1$ state, the azimuthal quantum number m being either -1, 0 or $+1$; the atom is exposed to a sinus square pulse of duration equal to 20 optical cycles, the frequency of the field being 0.25 a.u. The dashed line corresponds to the Floquet results and the markers to ours. The agreement between both results is impressive. However, in the case of $m=+1$, we observe some discrepancy when the electric field is larger than 0.4 a.u. (which is about six times the electric field on the $n=2$ orbit). This discrepancy is explained as follows: Zakrzewski and Delande calculations are

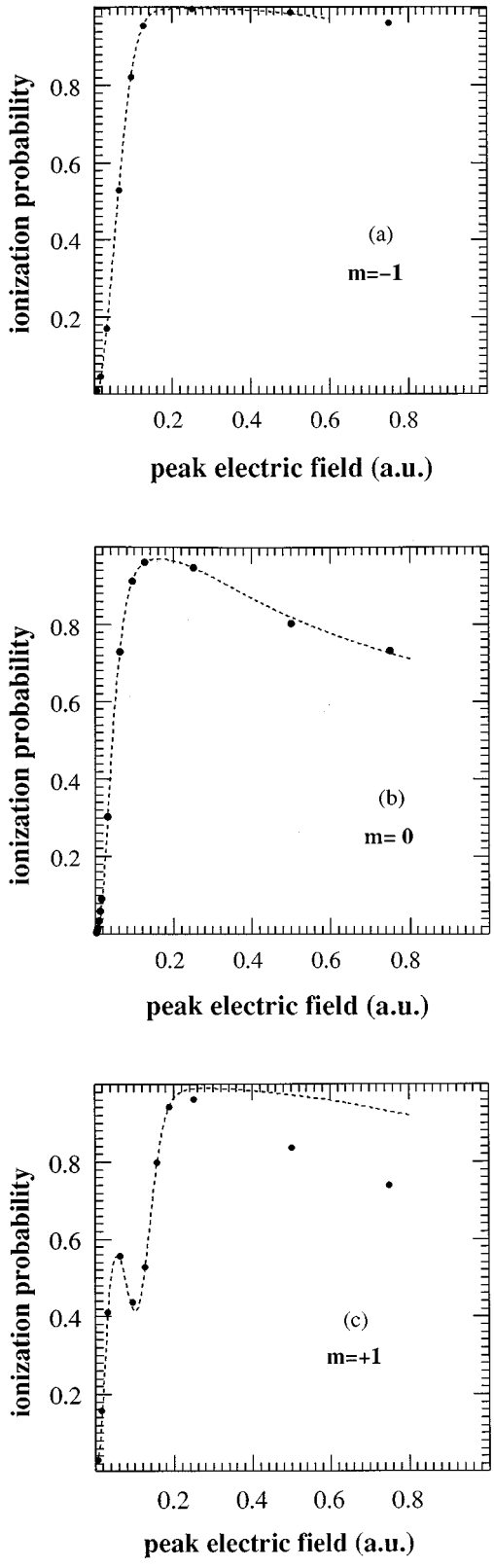

FIG. 8. Ionization probability as a function of the peak electric field in a.u. resulting from the interaction of atomic hydrogen with a sine square circularly polarized (σ^+) electromagnetic pulse of duration equal to 20 optical cycles. Atomic hydrogen is initially in an $n=2$, $l=1$ and (a) $m=-1$, (b) $m=0$, and (c) $m=+1$. The photon energy is 0.25 a.u. The dashed lines correspond to the results obtained by Zakrzewski and Delande by means of the single state Floquet approximation. The markers correspond to our results.

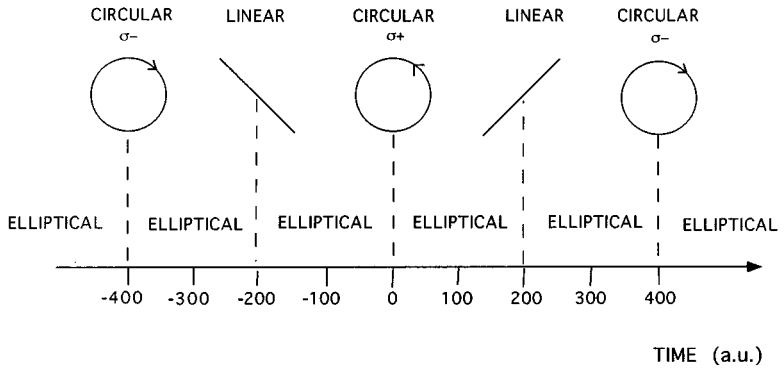

FIG. 9. Electric field polarization at some characteristic times in a.u. This electric field is obtained by superposing two perpendicular fields oscillating at two slightly different frequencies: $\omega_1=0.118$ and $\omega_2=0.110$ in a.u.

based on a single Floquet state approximation while we showed that in the present case [33], many states, in this intensity regime, are populated leading to the strong stabilization effect observed in Fig. 8(c).

VII. ILLUSTRATION

In this section, we consider the interaction of atomic hydrogen initially in its ground state with a pulsed electromagnetic field whose polarization depends on time. A time-dependent polarization may be achieved by superposing two perpendicular fields which oscillate at slightly different frequencies ω_1 and ω_2. The vector potential associated to such a field reads

$$\vec{A}(t)=A_0 f(t)[\cos(\omega_1 t)\vec{e}_x+\sin(\omega_2 t)\vec{e}_y], \qquad (27)$$

where A_0 is the amplitude of the vector potential, $\vec{e}_x$ and $\vec{e}_y$ the unit vectors along the x and y axis, respectively, and $f(t)$ a slowly varying time envelope. In the present case, it is a sine square function centered at time $t=0$ and starting at about $t=-500$ a.u. In all our calculations, we used the velocity form for the interaction Hamiltonian [34]. In Fig. 9, we show the electric field polarization at some characteristic times: at $t=\pm 400$ a.u., the polarization is circular (σ^- polarization), at $t=-200$ a.u., the polarization is linear with the field oscillation along the $y=-x$ axis, at $t=0$, polarization becomes circular again with the electric field rotating counterclockwise (σ^+ polarization) and finally, at $t=200$ a.u., the field is linearly polarized and oscillates along the $y=x$ axis; at other times, the polarization is elliptical. The calculations have been performed with a complex basis using 82 000 atomic states (40 angular momenta are included and 100 radial Sturmian functions for each l and m value). It is interesting to analyze the time step during the propagation of the solution. The results are presented in Fig. 10. At the beginning of the interaction, the time step is small because we impose the relative error on each component of the state vector Ψ to be of the order of 10^{-8}. We also observe that the time step decreases systematically when the polarization is circular. This is clear since while keeping the relative error of each component at the same level, the number of (l,m,n) states which are effectively accessed is much larger than in the case of linear polarization. When the field is linearly polarized, we know that high order harmonics are emitted [35]. Although the time step increases in that case it is kept more than one order of magnitude smaller than the optical period associated to the harmonic of the highest order.

In Fig. 11, we analyze as a function of time the ''1s-state population,'' namely, the projection of the full time-dependent wave function onto the bare 1s state of atomic hydrogen. Although the concept of stationary state loses its meaning during the time the system is interacting with the field, this quantity nevertheless gives information on the localization of the wave packet close to the nucleus at a given time. We see that this projection onto the bare 1s state exhibits fast oscillations at the average frequency $\overline{\omega}=(\omega_1+\omega_2)/2$ when the field is linearly polarized. In this case, the wave packet oscillates back and forth through the nucleus. The ''squeeze'' of the curve around $t=0$ and ± 400 a.u. arises because at these times, the polarization of the field is circular, preventing the oscillation of the wave packet through the nucleus.

VIII. CONCLUSIONS

We have described an approach of spectral type for numerically integrating the time-dependent Schrödinger equa-

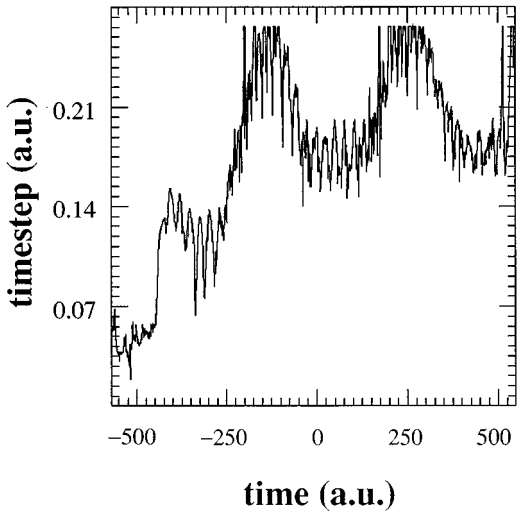

FIG. 10. Time step adjusted by the time propagation algorithm as a function of time in a.u. for the following case: atomic hydrogen initially in its ground state is exposed to a pulsed field whose polarization changes in time as described in Fig. 8. For both field components, the pulse envelope is flat with sine square two optical cycle turn on and off, the full duration being equal to 20 optical cycles. For both field components, the corresponding peak intensity is 10^{14} W/cm^2.

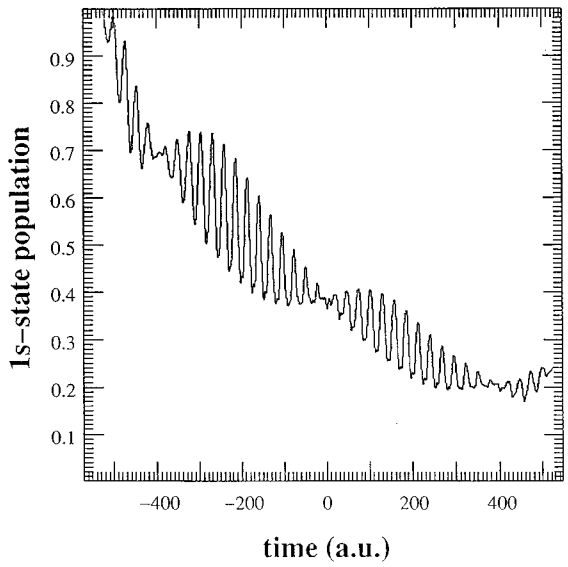

FIG. 11. Projection of the full time-dependent wave function on the bare 1*s* state of atomic hydrogen as a function of time in a.u. for the same case as described in Fig. 9.

tion associated to the interaction of a one active electron atom with an electromagnetic pulsed field whose polarization may be arbitrary. The wave function, represented on a Coulomb-Sturmian basis, is propagated by means of a parallel-iterated Runge-Kutta method. This method is in fact fully implicit and of very high order, ensuring a high stability of the time propagation. Moreover, it has the following advantages: it provides a scheme for an adaptive time step and it is particularly well suited to parallel computing. The method has been successfully used in many cases and where comparison was possible, our results are in good agreement with other calculations. So far, this method has turned out to be extremely efficient and enabled us to solve the time-dependent Schrödinger equation for the interaction of atomic hydrogen with a strong pulsed electromagnetic field of arbitrary polarization. The generalization of this method to the case of the Dirac equation for the treatment of relativistic effects in strong fields as well as to the case of the interaction of a two active electron atom with a laser pulse is presently in progress.

ACKNOWLEDGMENTS

One of us (B.P.) is supported in Belgium by the ''Fonds National de la Recherche Scientifique''; he thanks Robin Shakeshaft and Marcel Pont for their hospitality and for many fruitful discussions. All the computations have been performed on the SPP2 Convex supercomputer of the University of Louvain. M.G. is supported in part by the Catholic University of Louvain and by the Polish Commitee for Scientific Research under Grant No. 2P03B04209. The authors are grateful to Kuba Zakrzewski and Dominique Delande for providing them with numerical data. They thank P. J. van der Houwen and B. P. Sommeijer for many valuable discussions and for having provided them with a research code which was of great help for the development of the present method. Finally, very helpful discussions with A. Magnus and J. Meinguet are gratefully acknowledged.

APPENDIX: MATRIX ELEMENTS OF THE INTERACTION HAMILTONIAN

In this appendix, we give a list of the nonzero matrix elements $\langle S^{\kappa}_{n,l}|H^{V,L}_{\rm int}(\vec{r},t)|S^{\kappa}_{n',l'}\rangle$.

1. Velocity form

The interaction Hamiltonian in the velocity form is given by the following expression:

$$H^{V}_{\rm int}(\vec{r},t)=\frac{1}{c}\vec{A}(t)\cdot\vec{p}. \tag{A1}$$

For a field linearly polarized along the z axis, the vector potential can be written as

$$\vec{A}(t)=A_z(t)\vec{\epsilon}_z. \tag{A2}$$

The corresponding matrix elements of $H^{V}_{\rm int}$ are related to the overlap matrix of the Sturmian functions:

$$\begin{aligned}\langle S^{\kappa}_{n,l}Y_{l,m}|H^{V}_{\rm int}|S^{\kappa}_{n',l'}Y_{l',m'}\rangle &= -i\sqrt{\frac{4\pi}{3}}\kappa(n-n')\langle S^{\kappa}_{l,n}|S^{\kappa}_{l',n'}\rangle\frac{1}{c}A_z(t)\\ &\quad\times\langle l,m|Y_{1,0}|l',m'\rangle,\end{aligned} \tag{A3}$$

where $\langle l,m|Y_{1,0}|l',m'\rangle$ is the angular part of the matrix element.

The interaction couples states whose angular momenta differ by one, $|l-l'|=1$, but it does not mix states of different azimuthal quantum numbers m. The size of the Hamiltonian matrices depends only on the number of angular momenta and number of Sturmian functions taken into account. The diagonal blocks of the Hamiltonian, $l=l'$, have three-banded structure but for the off-diagonal blocks ($l=l'+1$ or $l=l'-1$) only diagonal and second lower diagonal elements are different from zero.

For a field of an arbitrary polarization in the x-y plane

$$\vec{A}(t)=A_x(t)\vec{\epsilon}_x+A_y(t)\vec{\epsilon}_y. \tag{A4}$$

The corresponding matrix elements of $H^{V}_{\rm int}$ read

$$\begin{aligned}\langle S^{\kappa}_{n,l}Y_{l,m}|H^{V}_{\rm int}|S^{\kappa}_{n',l'}Y_{l',m'}\rangle &= i\sqrt{\frac{2\pi}{3}}\kappa(n-n')\langle S^{\kappa}_{l,n}|S^{\kappa}_{l',n'}\rangle\left[\frac{1}{c}A^{-}(t)\langle l,m|Y_{1,1}|l',m'\rangle\right.\\ &\quad\left.-\frac{1}{c}A^{+}(t)\langle l,m|Y_{1,-1}|l',m'\rangle\right]\end{aligned} \tag{A5}$$

where $A^{+}(t)$ and $A^{-}(t)$ are defined as

$$A^{+}(t)=A_x(t)+iA_y(t), \tag{A6}$$

$$A^{-}(t)=A_x(t)-iA_y(t). \tag{A7}$$

The interaction couples not only states of different angular momentum, $|l-l'|=1$, but also mixes states of different azimuthal quantum numbers, $|m-m'|=1$. The off-diagonal blocks ($l\neq l'$) can be divided into subblocks corresponding to different azimuthal quantum numbers m and m'. The off-diagonal blocks are no longer square matrices as the number of different m values depends on the angular momentum l. The size of the Hamiltonian matrices depends on the number of Sturmian functions, on the number of angular momenta taken into account as well as on the number of involved azimuthal quantum numbers for a given angular momentum; therefore it grows quadratically with l. Below, we give a list of matrix elements of the overlap matrix wich are needed for the construction of the Hamiltonian matrix.

Diagonal blocks:

$$\langle S^{\kappa}_{n,l}|S^{\kappa}_{n,l}\rangle=1, \tag{A8}$$

$$\langle S^{\kappa}_{n,l}|S^{\kappa}_{n+1,l}\rangle=-\frac{1}{2}\sqrt{\frac{(n+l+1)(n-l)}{n(n+1)}}, \tag{A9}$$

$$\langle S^{\kappa}_{n,l}|S^{\kappa}_{n-1,l}\rangle=-\frac{1}{2}\sqrt{\frac{(n+l)(n-l-1)}{n(n-1)}}. \tag{A10}$$

Off-diagonal blocks:

$$\langle S^{\kappa}_{n,l}|S^{\kappa}_{n+1,l+1}\rangle=\frac{1}{2}\sqrt{\frac{(n+l+1)(n+l+2)}{n(n+1)}}, \tag{A11}$$

$$\langle S^{\kappa}_{n,l}|S^{\kappa}_{n,l+1}\rangle=-\sqrt{\frac{(n+l+1)(n-l-1)}{n^2}}, \tag{A12}$$

$$\langle S^{\kappa}_{n,l}|S^{\kappa}_{n-1,l+1}\rangle=\frac{1}{2}\sqrt{\frac{(n-l-1)(n-l-2)}{n(n-1)}}, \tag{A13}$$

$$\langle S^{\kappa}_{n,l}|S^{\kappa}_{n+1,l-1}\rangle=\frac{1}{2}\sqrt{\frac{(n-l)(n-l+1)}{n(n+1)}}, \tag{A14}$$

$$\langle S^{\kappa}_{n,l}|S^{\kappa}_{n,l-1}\rangle=-\sqrt{\frac{(n+l)(n-l)}{n^2}}, \tag{A15}$$

$$\langle S^{\kappa}_{n,l}|S^{\kappa}_{n-1,l+1}\rangle=\frac{1}{2}\sqrt{\frac{(n+l)(n+l-1)}{n(n-1)}}. \tag{A16}$$

2. Length form

The interaction Hamiltonian in the length form is given by the following expression:

$$H^{L}_{\rm int}(\vec{r},t)=\vec{E}(t)\cdot\vec{r}. \tag{A17}$$

For a field linearly polarized along the z axis, we have

$$\vec{E}(t)=E_z(t)\vec{\epsilon}_z. \tag{A18}$$

The corresponding matrix elements of the $H^{L}_{\rm int}$ are

$$\langle S^{\kappa}_{n,l}Y_{l,m}|H^{L}_{\rm int}|S^{\kappa}_{n',l'}Y_{l',m'}\rangle=E_z(t)\sqrt{\frac{4\pi}{3}}\langle S^{\kappa}_{l,n}|r|S^{\kappa}_{l',n'}\rangle \times\langle l,m|Y_{1,0}|Y_{l',m'}\rangle. \tag{A19}$$

For a field of an arbitrary polarization in the x-y plane

$$\vec{E}(t)=E_x(t)\vec{\epsilon}_x+E_y(t)\vec{\epsilon}_y. \tag{A20}$$

The corresponding matrix elements of $H^{L}_{\rm int}$ read

$$\langle S^{\kappa}_{n,l}Y_{l,m}|H^{L}_{\rm int}|S^{\kappa}_{n',l'}Y_{l',m'}\rangle =-\sqrt{\frac{2\pi}{3}}\langle S^{\kappa}_{l,n}|r|S^{\kappa}_{l',n'}\rangle[E^{-}(t)\langle l,m|Y_{1,1}|l',m'\rangle -E^{+}(t)\langle l,m|Y_{1,-1}|l',m'\rangle], \tag{A21}$$

where $E^{+}(t)$ and $E^{-}(t)$ are defined as

$$E^{+}(t)=E_x(t)+iE_y(t), \tag{A22}$$

$$E^{-}(t)=E_x(t)-iE_y(t). \tag{A23}$$

As it follows from the above expressions the Hamiltonian is given in terms of the matrix elements of the position operator in the Sturmian basis. Below, we present the list of the non-vanishing elements:

$$\langle S^{\kappa}_{n,l}|r|S^{\kappa}_{n+2,l+1}\rangle =-\frac{1}{4\kappa}\sqrt{\frac{(n-l-1)(n-l-2)(n-l-3)(n+l)}{n(n-2)}}, \tag{A24}$$

$$\langle S^{\kappa}_{n,l}|r|S^{\kappa}_{n+1,l+1}\rangle=\frac{1}{2\kappa}(2n-l)\sqrt{\frac{(n+l+1)(n+l+2)}{n(n+1)}}, \tag{A25}$$

$$\langle S^{\kappa}_{n,l}|r|S^{\kappa}_{n,l+1}\rangle=-\frac{3}{2\kappa}\sqrt{(n-l-1)(n+l+1)}, \tag{A26}$$

$$\langle S^{\kappa}_{n,l}|r|S^{\kappa}_{n-1,l+1}\rangle=\frac{1}{2\kappa}(2n+l)\sqrt{\frac{(n-l-1)(n-l-2)}{n(n-1)}}, \tag{A27}$$

$$\langle S^{\kappa}_{n,l}|r|S^{\kappa}_{n-2,l+1}\rangle =-\frac{1}{4\kappa}\sqrt{\frac{(n-l-1)(n-l-2)(n-l-3)(n+l)}{n(n-2)}}, \tag{A28}$$

$$\langle S^{\kappa}_{n,l}|r|S^{\kappa}_{n+2,l-1}\rangle =-\frac{1}{4\kappa}\sqrt{\frac{(n-l+2)(n-l+1)(n-l)(n+l+1)}{n(n+2)}}, \tag{A29}$$

$$\langle S^{\kappa}_{n,l}|r|S^{\kappa}_{n+1,l-1}\rangle=\frac{1}{2\kappa}(2n+l+1)\sqrt{\frac{(n-l+1)(n-l)}{n(n+1)}}, \tag{A30}$$

$$\langle S^{\kappa}_{n,l}|r|S^{\kappa}_{n,l+1}\rangle = -\frac{3}{2\kappa}\sqrt{(n-l)(n+l)}, \tag{A31}$$

$$\langle S^{\kappa}_{n,l}|r|S^{\kappa}_{n-1,l-1}\rangle = \frac{1}{2\kappa}(2n-l-1)\sqrt{\frac{(n+l-1)(n+l)}{n(n-1)}}, \tag{A32}$$

$$\langle S^{\kappa}_{n,l}|r|S^{\kappa}_{n+2,l-1}\rangle = -\frac{1}{4\kappa}\sqrt{\frac{(n+l-2)(n+l-1)(n+l)(n-l-1)}{n(n-2)}}. \tag{A33}$$

[1] The first large scale numerical simulations based on time-dependent methods have been carried out in scattering theory. See, e.g., H. Kröger, Phys. Rep. **210**, 45 (1992).

[2] See, e.g., the *Proceedings of the NATO Advanced Research Workshop, Super Intense Laser Atom Physics (SILAP III)*, Vol. 316 of *NATO Advanced Study Institute Series B: Physics*, edited by B. Piraux, A. L'Huillier, and K. Rzążewski (Plenum, New York, 1993).

[3] K. C. Kulander, K. J. Schafer, and J. L. Krause, Phys. Rev. Lett. **66**, 2601 (1991).

[4] P. J. van der Houwen, B. P. Sommeijer, and W. Couzy, Math. Comp. **58**, 135 (1992).

[5] A. Bugacov, M. Pont, R. Shakeshaft, and B. Piraux, Phys. Rev. A **51**, 1490 (1995); A. Bugacov, B. Piraux, M. Pont, and R. Shakeshaft, *ibid.* **51**, 4877 (1995).

[6] M. Gajda, B. Piraux, and K. Rzążewski (unpublished).

[7] Grid methods are now widely used. See, e.g., C. Cerjan and K. Kulander, Comput. Phys. Commun. **63**, 529 (1991).

[8] L. A. Collins and A. L. Merts, Phys. Rev. A **40**, 4127 (1989); X. Tang, H. Rudolph, and P. Lambropoulos, Phys. Rev. Lett. **65**, 3269 (1990); M. Pont, D. Proulx, and R. Shakeshaft, Phys. Rev. A **44**, 4486 (1991).

[9] K. C. Kulander, Phys. Rev. A **35**, 445 (1987).

[10] See, e.g., *Atoms in Intense Laser Fields*, Advances in Atomic, Molecular, and Optical Physics, Supplement 1, edited by M. Gavrila (Academic Press, Inc., London, 1992).

[11] E. Hairer and G. Wanner, in *Solving Ordinary Differential Equations II: Stiff and Differential-Algebraic Problems* (Springer-Verlag, Berlin, 1991).

[12] X. Tang, H. Rudolph, and P. Lambropoulos, Phys. Rev. Lett. **65**, 3269 (1990).

[13] M. Pont, D. Proulx, and R. Shakeshaft, Phys. Rev. A **44**, 4486 (1991).

[14] H. A. Yamani and W. P. Reinhardt, Phys. Rev. A **11**, 1144 (1975).

[15] R. Courant and D. Hilbert, in *Methods of Mathematical Physics* (Interscience Publishers, New York, 1953), p. 291.

[16] C. De Boor, *A Practical Guide to Splines* (Springer-Verlag, Berlin, 1978).

[17] E. Cormier and P. Lambropoulos, J. Phys. B **29**, 1667 (1996); see also E. Cormier, Ph.D. thesis, Université de Bordeaux I, 1994.

[18] Complex basis functions have been used previously to minimize reflections in time propagation. See W. P. Reinhardt, Annu. Rev. Phys. Chem. **33**, 223 (1982); C. W. McCurdy and S. D. Parker, Chem. Phys. Lett. **156**, 483 (1989); C. W. McCrudy and C. K. Stroud, Comput. Phys. Commun. **63**, 323 (1991); M. Pont, D. Proulx, and R. Shakeshaft, Phys. Rev. A **44**, 4486 (1991).

[19] R. M. Potvliege and R. Shakeshaft, Phys. Rev. A **40**, 3061 (1989).

[20] In the case where the Sturmian basis is real, such a radius cannot be defined rigorously since the range of a given linear superposition of Sturmian functions depends on the corresponding atomic energy in the continuum. By contrast, such a radius can be uniquely defined in the case of the spline functions; see, e.g., E. Cormier Ph.D. thesis, Université de Bordeaux I, 1994.

[21] B. Piraux and R. Shakeshaft, Phys. Rev. A **49**, 3903 (1994).

[22] M. Rotenberg, Adv. At. Mol. Phys. **6**, 233 (1970).

[23] P. Dean, Rev. Mod. Phys. **44**, 127 (1972).

[24] J. S. Dehesa, F. Dominguez Adame, E. R. Arriola, and A. Zarzo, in *Proceedings of the Third International Symposium on Orthogonal Polynomials and their Applications*, edited by C. Brezinski, L. Gori, and A. Ronveaux (J.C. Baltzer AG, Scientific Publishing Company, Basel, Switzerland, 1991), p. 223.

[25] P. J. van der Houwen and B. P. Sommeijer, SIAM J. Sci. Stat. Comput. **12**, 1000 (1991).

[26] J. D. Lambert, *Numerical Methods for Ordinary Differential Systems: The Initial Value Problem* (John Wiley & Sons, Chichester, 1991).

[27] See, e.g., W. H. Press, S. A. Teukolsky, W. T. Vetterling, and B. P. Flannery, *Numerical Recipes* (Cambridge University Press, Cambridge, England, 1992).

[28] R. Alexander, SIAM J. Numer. Anal. **14**, 1006 (1977).

[29] For a recent review see R. W. Freund, G. H. Golub, and N. M. Nachtigal, Acta Numerica **1991**, 57.

[30] For relatively high frequencies, it has been shown that harmonics of the driving field are essentially emitted at the beginning of the interaction of the atom with the external field; see Ph. Antoine, B. Piraux, and A. Maquet, Phys. Rev. A **51**, R1750 (1995).

[31] A. Maquet (private communication).

[32] J. Zakrzewski and D. Delande, J. Phys. B **28**, L667 (1995).

[33] M. Gajda, B. Piraux, and K. Rzążewski, Phys. Rev. A **50**, 2528 (1994).

[34] The reason the velocity form is more convenient than the length form has been discussed in detail by R. Shakeshaft, Z. Phys. D **6**, 47 (1988); see also E. Cormier and P. Lambropoulos, J. Phys. B **29**, 1667 (1996).

[35] Ph. Antoine, B. Piraux, D. B. Milošević, and M. Gajda, Phys. Rev. A **54**, 1761 (1996).